ALICE Status Report

Ante Bilandzic, ALICE Collaboration
Technical University of Munich

“151st LHCC Meeting”, CERN, 14/09/2022

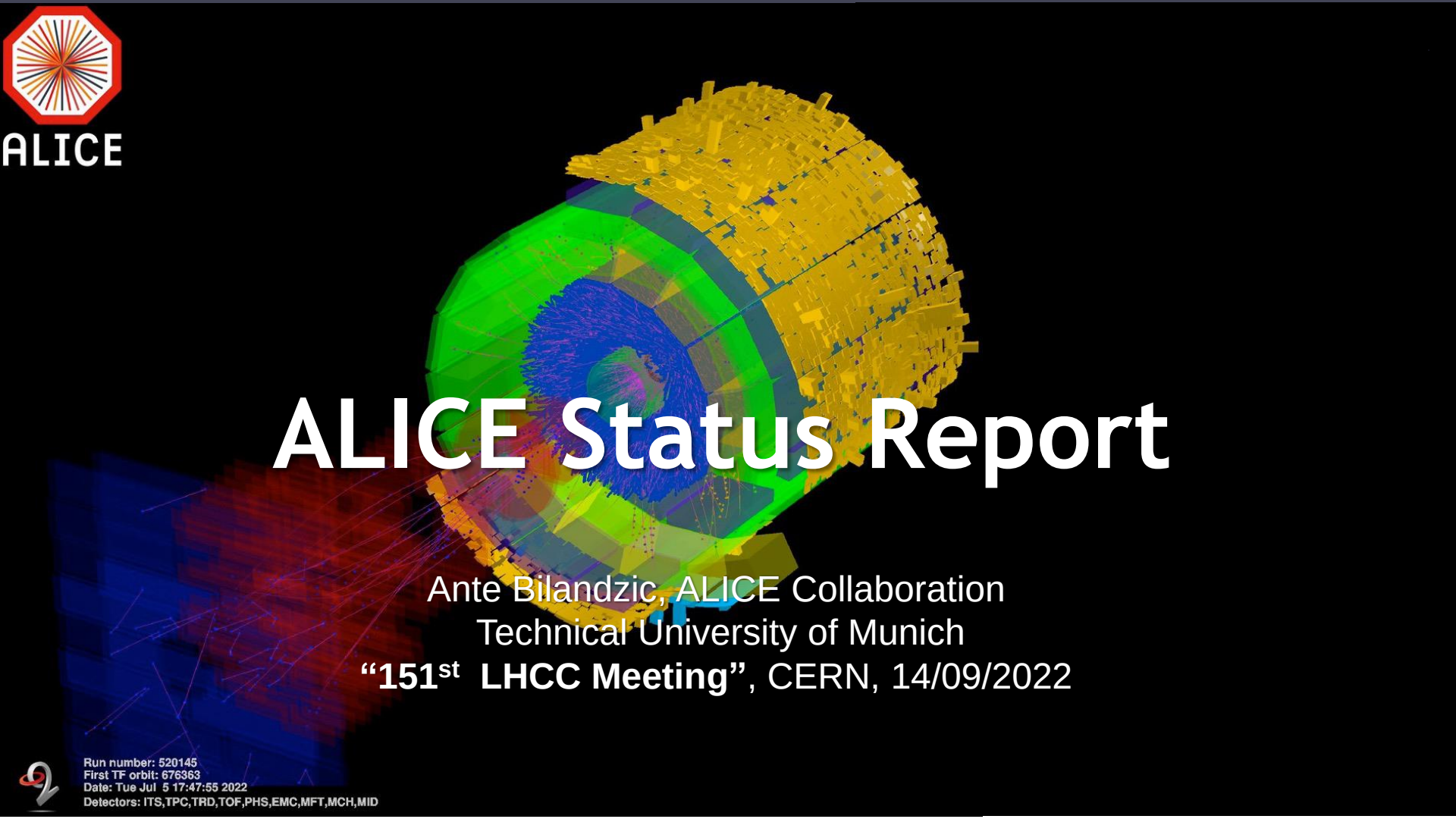

European Research Council
Established by the European Commission

Outline

- Latest publications
- Run 3
- Future upgrades

Latest publications

Latest publications

Submitted (since last LHCC in June):

1. "Towards the understanding of the genuine three-body interaction for $\mathrm{p-p-p}$ and $\mathrm{p-p-\Lambda}$" (CDS / arXiv:2206.03344)
2. "Closing in on critical net-baryon fluctuations at LHC energies: cumulants up to third order in Pb−Pb collisions" (CDS / arXiv:2206.03343)
3. "Observation of flow angle and flow magnitude fluctuations in Pb−Pb collisions at $\sqrt{s_{NN}} = 5.02$ TeV at the LHC" (CDS / arXiv:2206.04574)
4. "Anisotropic flow and flow fluctuations of identified hadrons in Pb−Pb collisions at $\sqrt{s_{NN}} = 5.02$ TeV" (CDS / arXiv:2206.04587)
5. "$f_0(980)$ production in inelastic pp collisions at $\sqrt{s_{NN}} = 5.02$ TeV" (CDS / arXiv:2206.06216)
6. "Measurements of groomed-jet substructure of charm jets tagged by D^0 mesons in proton-proton collisions at $\sqrt{s} = 13$ TeV" (CDS / arXiv:2208.04857)
7. "Multiplicity dependence of Y production at forward rapidity in pp collisions at $\sqrt{s_{NN}} = 13$ TeV" (CDS / arXiv:2209.04241)
8. "Performance of the ALICE Electromagnetic Calorimeter" (CDS / arXiv:2209.04216)
9. "Neutron emission in ultraperipheral Pb–Pb collisions at $\sqrt{s_{NN}} = 5.02$ TeV" (CDS / arXiv:2209.04250)

Major conferences:

ICHEP 2022 BOLOGNA

- 1 plenary talk
- 39 parallel talks
- 13 posters

Heavy-ion collisions and QCD phase diagram

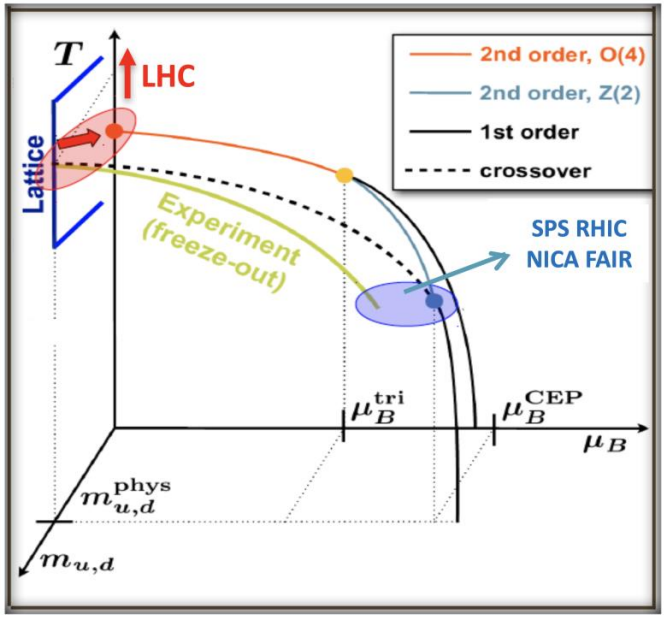

F. Karsch, Schleching 2016

- Phase diagram of strongly interacting nuclear matter can be explored in ultrarelativistic heavy-ion collisions
- State of quark–gluon plasma is probed as a function of temperature and baryon chemical potential

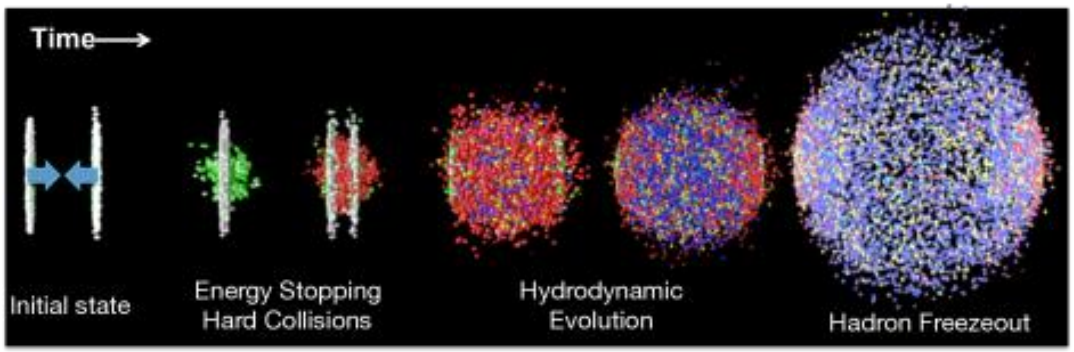

Nature of phase transition

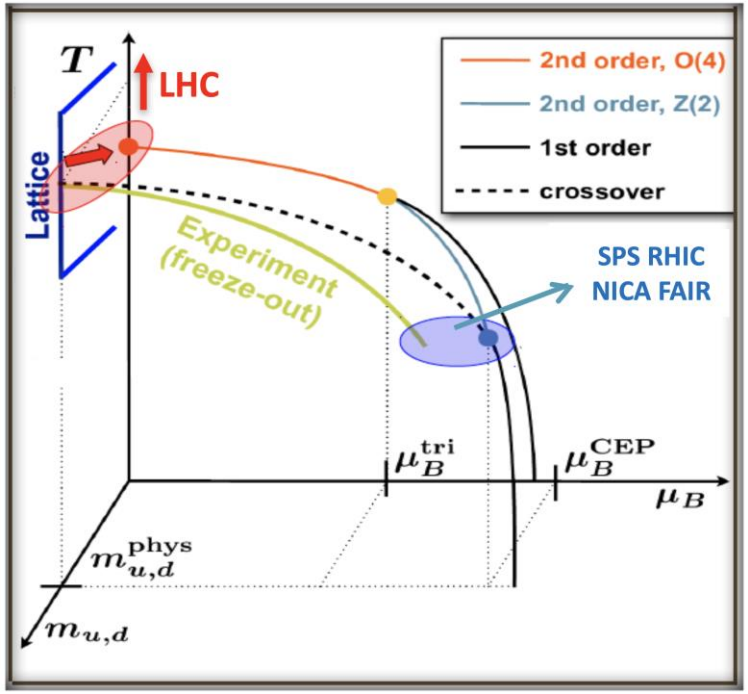

F. Karsch, Schleching 2016

$$\chi_{klmn}^{B,S,Q,C} = \frac{\partial^{(k+l+m+n)}(P(\hat{\mu}_B,\hat{\mu}_S,\hat{\mu}_Q,\hat{\mu}_C)/T^4)}{\partial\hat{\mu}_B^k\partial\hat{\mu}_S^l\partial\hat{\mu}_Q^m\partial\hat{\mu}_C^n}\Big|_{\vec{\mu}=0}$$

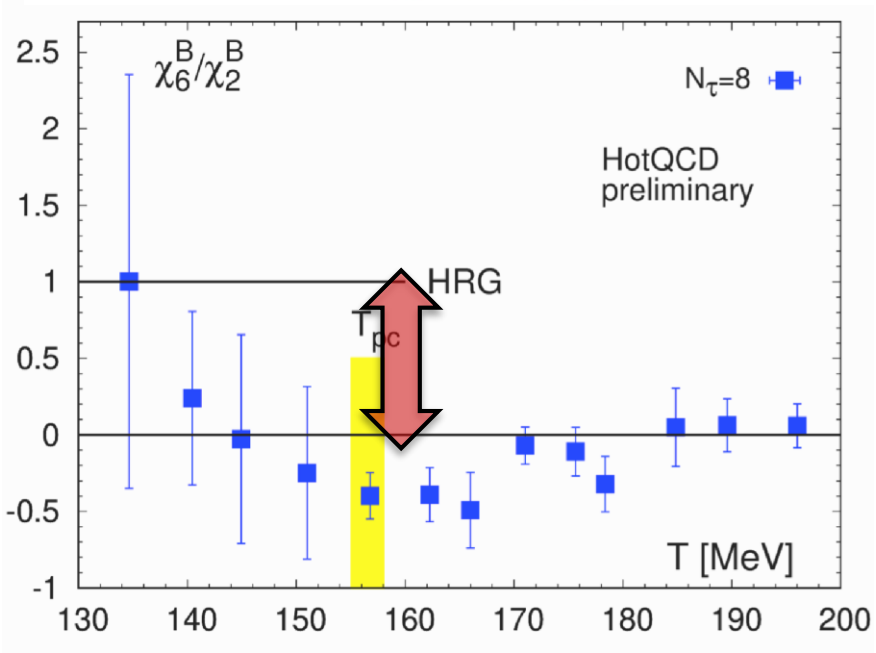

- The properties of the QCD phase transition depend on the number of quark flavors and their masses
- Signs of criticality – starting only with 6th order cumulants of net-charge distributions

2nd order cumulants of net-protons

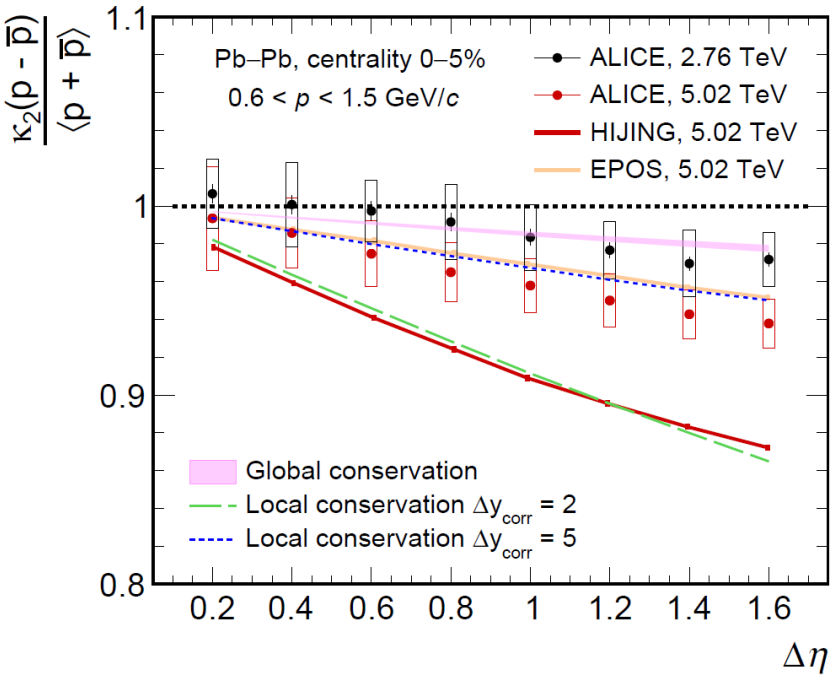

Experiment:

$$\Delta N_B = X = N_B - N_{\bar{B}}$$

$\kappa_n \rightarrow$ cumulants (i.e. $\kappa_2 \equiv \langle X^2 \rangle - \langle X \rangle^2$)

$$\hat{c}_2^B = \frac{k_2(DN_B)}{VT^3} \Rightarrow \frac{k_4(DN_B)}{k_2(DN_B)} = \frac{\hat{c}_4^B}{\hat{c}_2^B}$$

- Deviation from Skellam baseline is due to baryon number conservation
- ALICE data suggest long range correlations, $\Delta y = \pm 2.5$ unit or longer → earlier in time
  A. Dumitru et al., Nucl. Phys. A 810 (2008) 91
- EPOS agrees with ALICE data but HIJING deviates significantly
  - Event generators based on string fragmentation (HIJING) conserve baryon number over $\Delta y = \pm 1$ unit

"Closing in on critical net-baryon fluctuations at LHC energies: cumulants up to third order in Pb−Pb collisions" (CDS / arXiv:2206.03343)

3rd order cumulants of net-protons

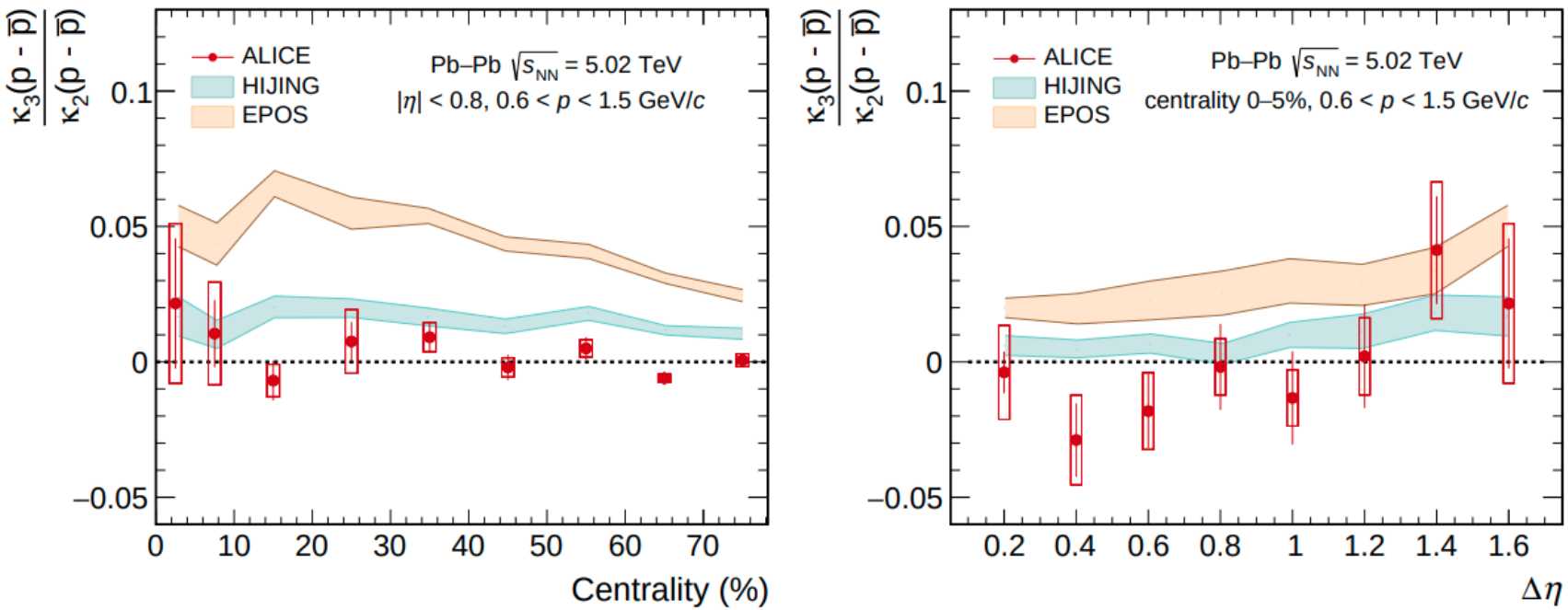

- Data agree with Skellam baseline "0" as a function of centrality and pseudorapidity
  - Up to **3rd order** ALICE data agree with the LQCD expectations
  - μ_B is very close to 0 at LHC energies
- EPOS and HIJING deviate from "0"
  - They conserve global charge but $p/\bar{p}$ deviates from unity:
    1.025 ± 0.004 (EPOS), 1.008 ± 0.002 (HIJING)

"Closing in on critical net-baryon fluctuations at LHC energies: cumulants up to third order in Pb−Pb collisions" (CDS / arXiv:2206.03343)

Collective phenomena

- Properties of quark–gluon plasma (QGP) can be probed by analysing collective phenomena in heavy-ion collisions with multiparticle analysis techniques

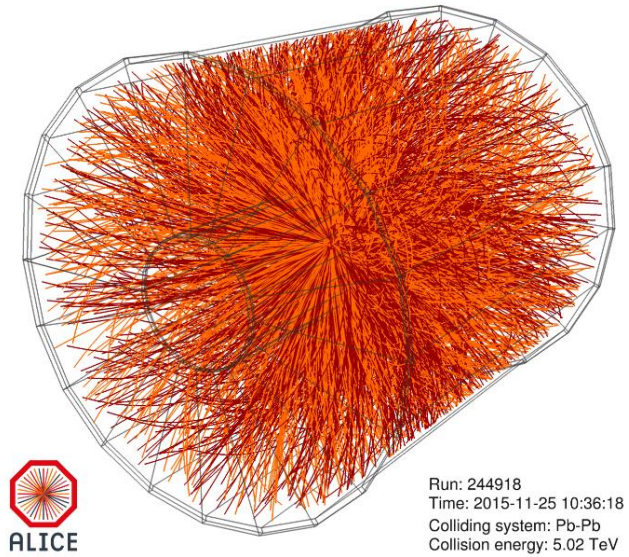

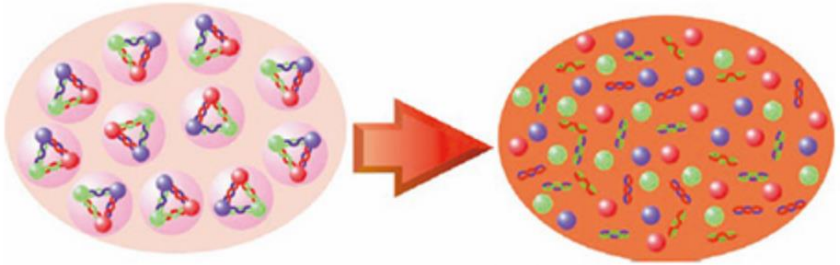

P. F. Kolb, U. W. Heinz, nucl-th/0305084

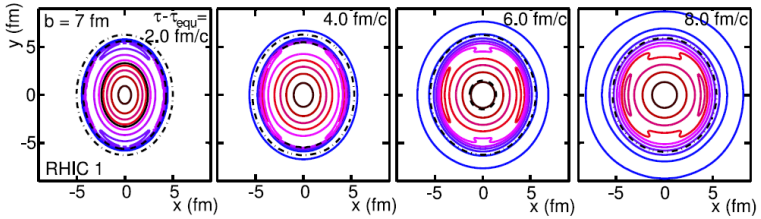

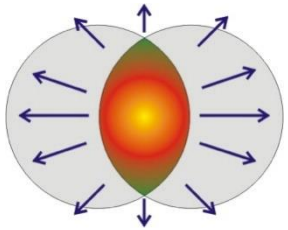

Open questions:

- How to seperate initial-state effects from QGP transport properties in measured observables?
- What are the smallest collision systems in which QGP can be formed?
- What is origin of observed universality of flow measurements in different collision systems?

Flow angle and magnitude fluctuations

- Are symmetry planes the same for all particles, irrespective of their p_T ?
- First observation of flow angle fluctuations:

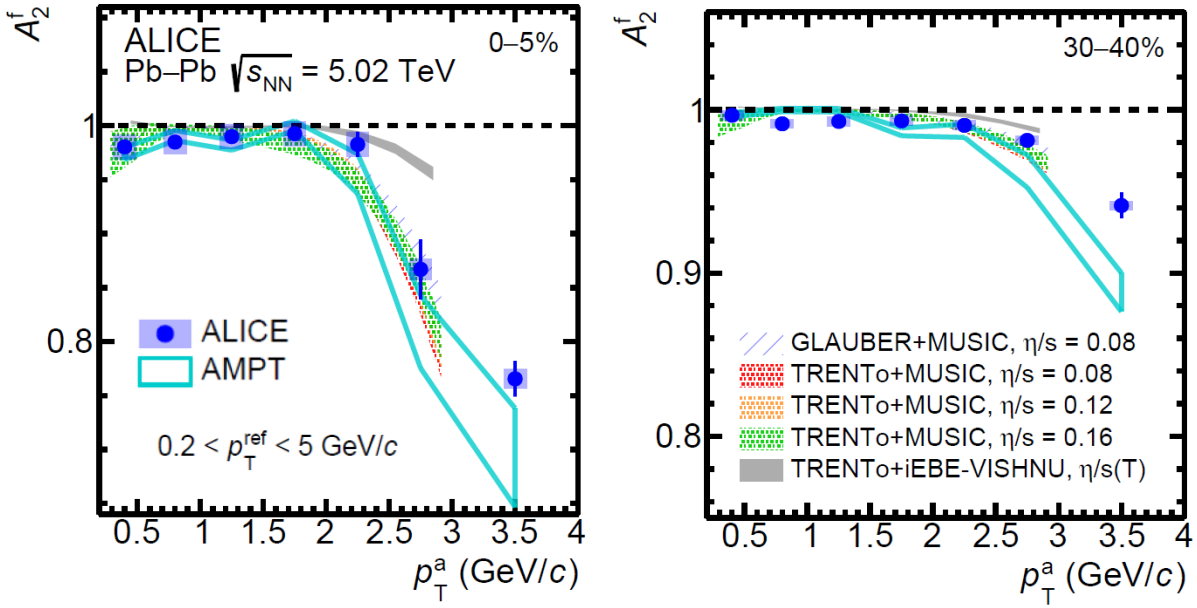

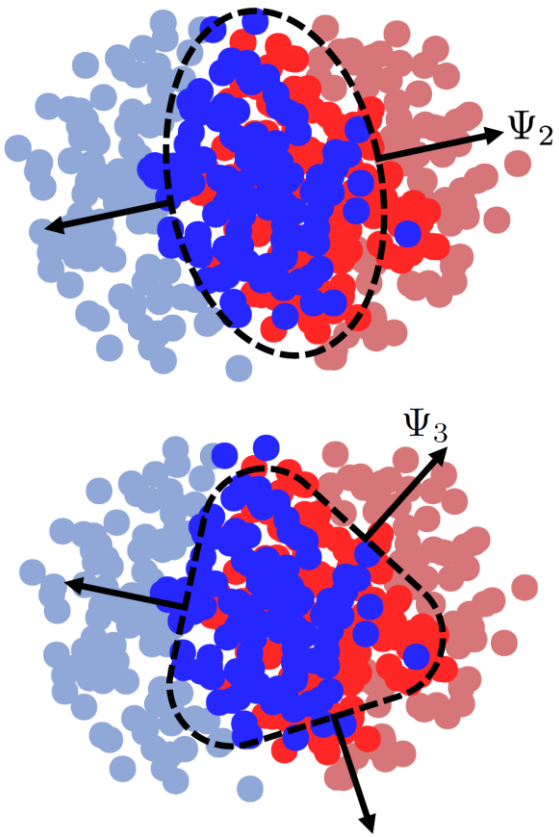

$$A_n^f = \frac{\langle\langle \cos n[\varphi_1^a + \varphi_2^a - \varphi_3 - \varphi_4]\rangle\rangle}{\langle\langle \cos n[\varphi_1^a + \varphi_2 - \varphi_3^a - \varphi_4]\rangle\rangle} = \frac{\langle v_n^2(p_T^a)\, v_n^2 \cos 2n[\Psi_n(p_T^a) - \Psi_n]\rangle}{\langle v_n^2(p_T^a) v_n^2\rangle}$$

$$\simeq \langle \cos 2n[\Psi_n(p_T^a) - \Psi_n]\rangle_w,$$

- Effect most pronounced at high p_T

"Observation of flow angle and flow magnitude fluctuations in Pb−Pb collisions at $\sqrt{s_{NN}}$ = 5.02 TeV at the LHC" (CDS / arXiv:2206.04574)

Flow of identified hadrons

- Elliptic flow estimated with 4-particle cumulants, $v_2\{4\}$, for identified hadrons:

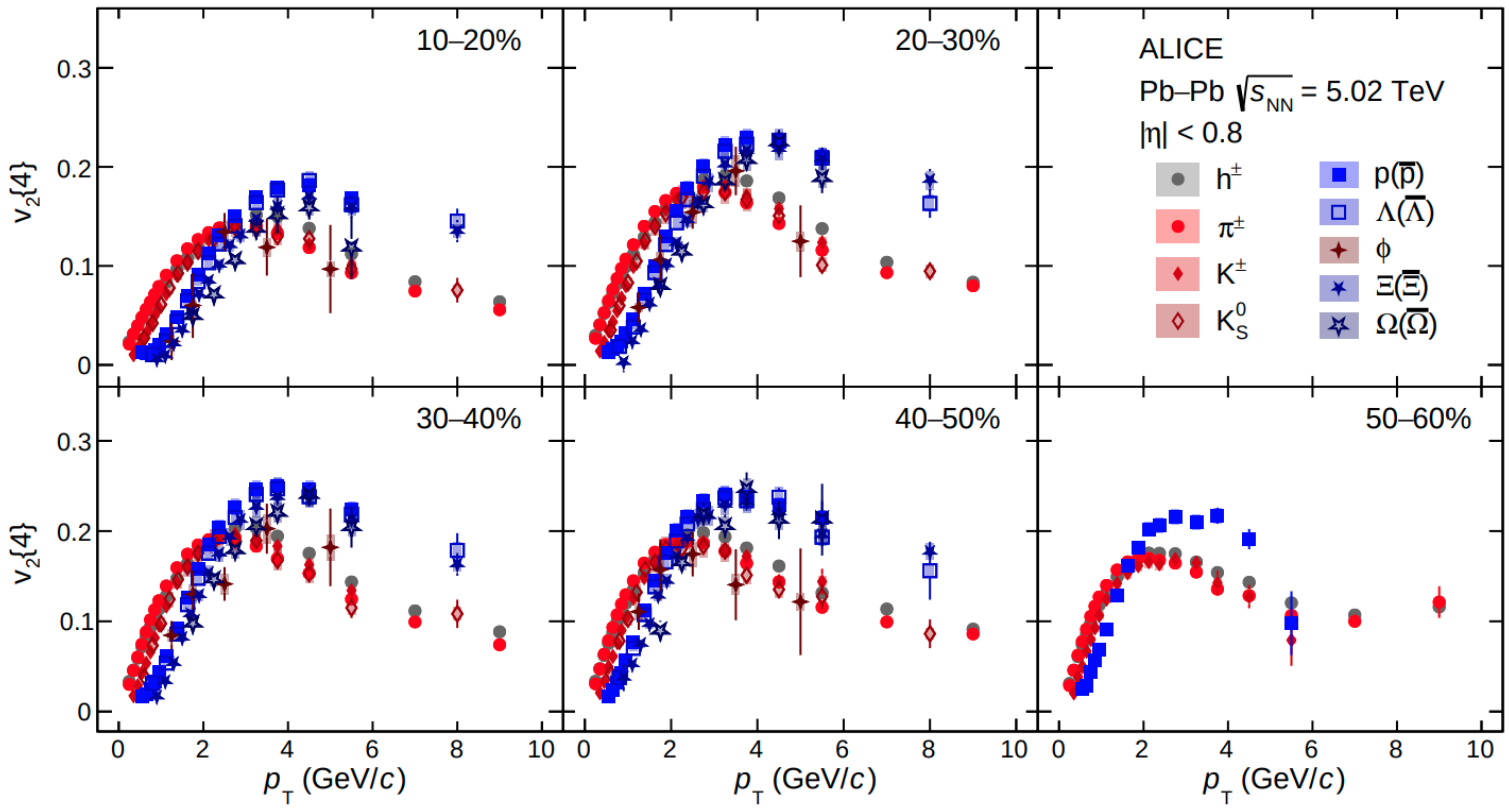

- Confirmed mass ordering at low p_T and particle-type grouping (mesons vs. baryons at intermediate p_T)

"Anisotropic flow and flow fluctuations of identified hadrons in Pb−Pb collisions at $\sqrt{s_{NN}}$ = 5.02 TeV" (CDS / arXiv:2206.04587)

Neutron emission in ultraperipheral collisions

- Study of photon-induced reactions in ultraperipheral collisions (UPC)
- Electromagnetic dissociation in UPC leads to the production of neutrons at beam rapidities

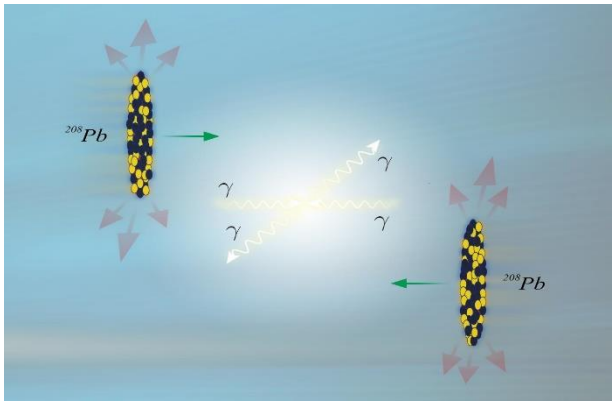

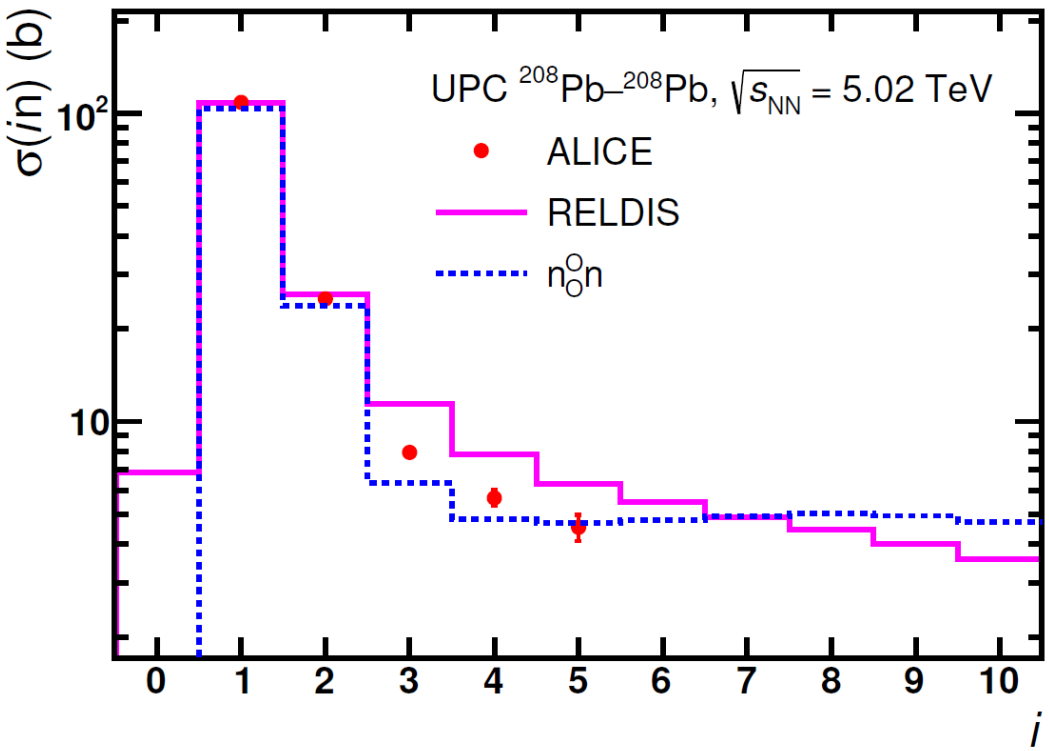

- Models describe data well only for 1n and 2n cross sections
- This measurement is valuable input for simulations of secondary ion beams at HL-LHC and FCC

"Neutron emission in ultraperipheral Pb–Pb collisions at $\sqrt{s_{NN}}$ = 5.02 TeV"

(CDS / arXiv:2209.04250)

A wider range of QCD studies…

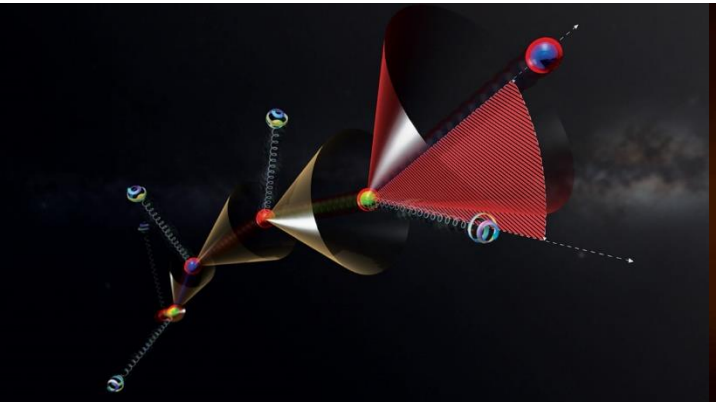

Jet fragmentation

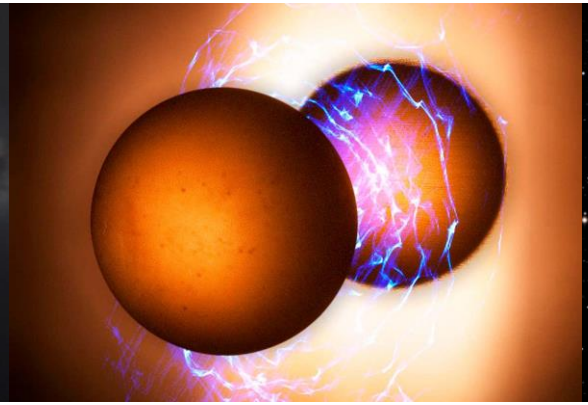

Strong nuclear force

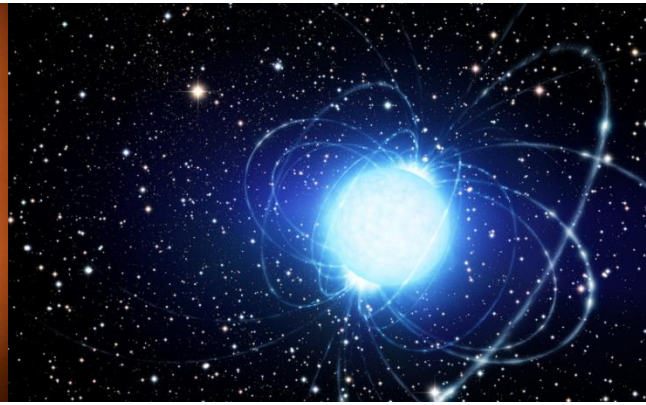

Neutron stars

Nuclear matter

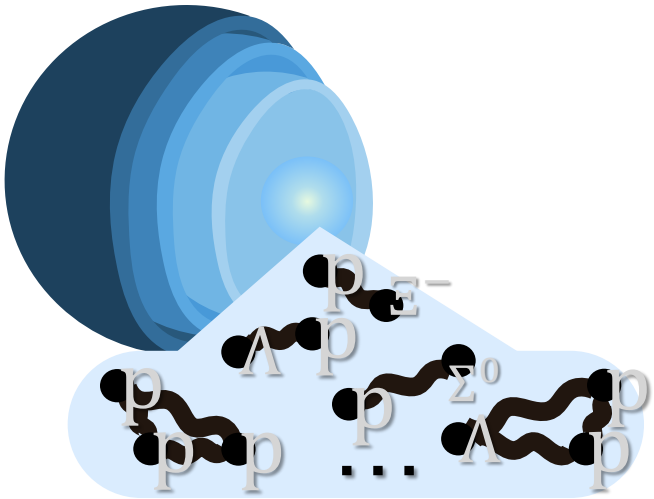

- Properties of nuclei and hypernuclei cannot be described satisfactorily with two-body forces only

  L.E. Marcucci et al., Front. Phys. 8:69 (2020)

- N-N-N and N-N-Λ interactions: fundamental ingredients for the Equation of State (EoS) of neutron stars

  D. Lonardoni et al., PRL 114, 092301 (2015)

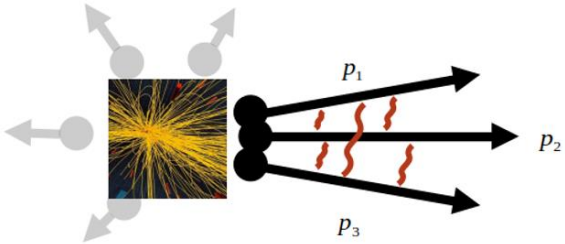

Femtoscopic technique

- Genuine multiparticle correlations, or cumulants, can be isolated from the measured multiparticle correlations with the Kubo's formalism:

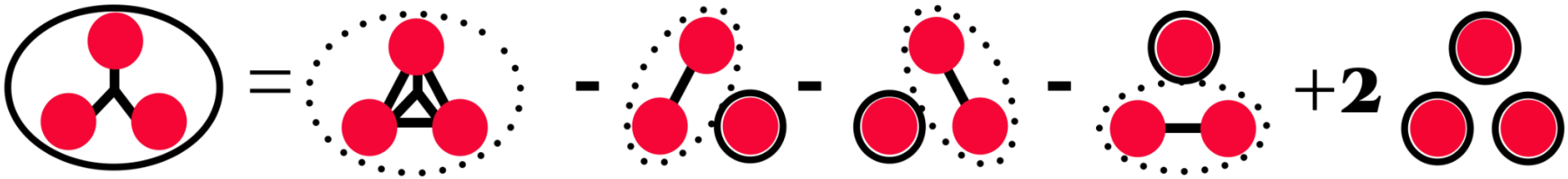

Genuine 3-body correlation

3-body correlation

2-body correlation + permutations

Non-interacting particles

R. Kubo, J. Phys. Soc. Jpn. ***17****(7), 1100 (1962)*

3-body correlation functions

- Measured three-particle correlation functions deviate from lower-order contributions, hinting to three-body effects

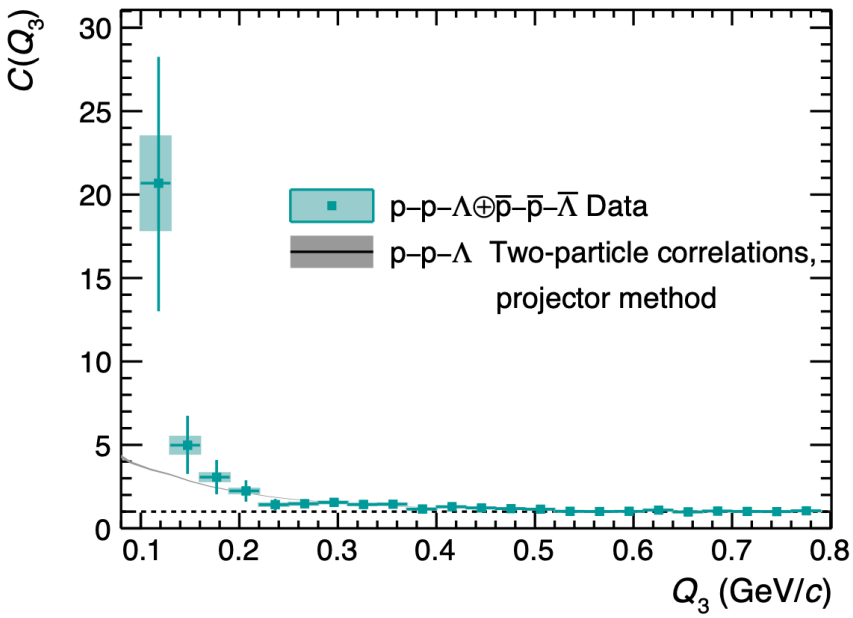

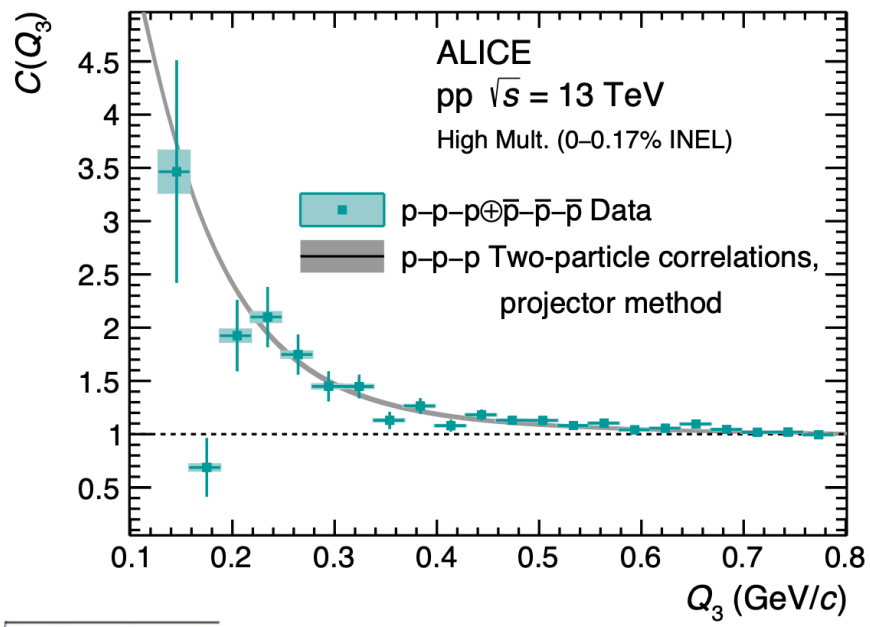

$$Q_3 = \sqrt{-q_{ij}^2 - q_{jk}^2 - q_{ki}^2}$$

Statistical significance:

p-p-Λ: $n_\sigma = 0.8$ **for** $Q_3 < 0.4$ **GeV/**c

p-p-p: $n_\sigma = 6.7$ **for** $Q_3 < 0.4$ **GeV/**c

"Towards the understanding of the genuine three-body interaction for p−p−p and p−p−Λ"
(CDS / arXiv:2206.03344)

First measurement of $f_0(980)$ production at LHC

- What is the strangeness content of $f_0(980)$?
- Is $f_0(980)$ quark-antiquark pair, tetraquark, or meson-meson molecule?

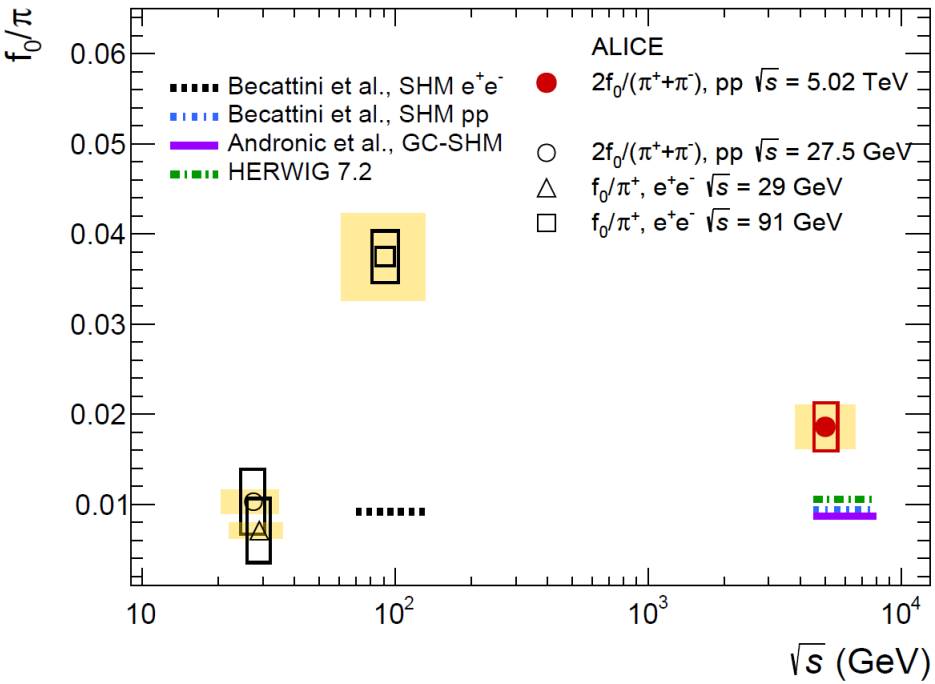

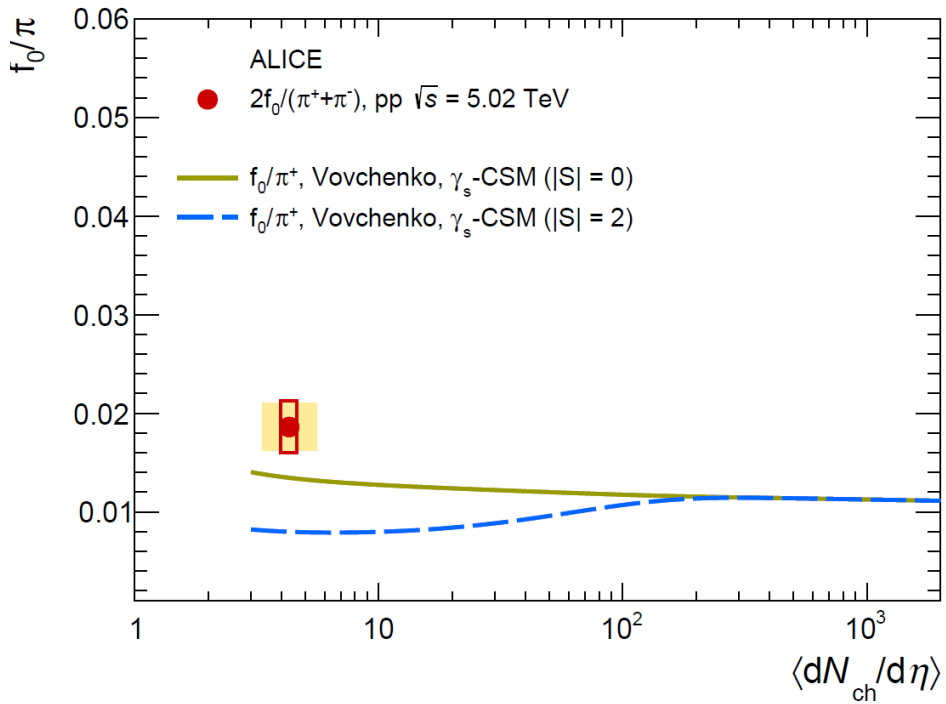

- From SPS to LHC: mild dependence of $f_0(980)$ to pion production in pp collisions
- All models underestimate p_T-integrated $f_0(980)$ yield
- No strangeness content is favoured by statistical models (to be ctd. in p–Pb and Pb–Pb)

"$f_0(980)$ production in inelastic pp collisions at $\sqrt{s_{NN}}$ = 5.02 TeV" (CDS / arXiv:2206.06216)

Charm-quark splitting function

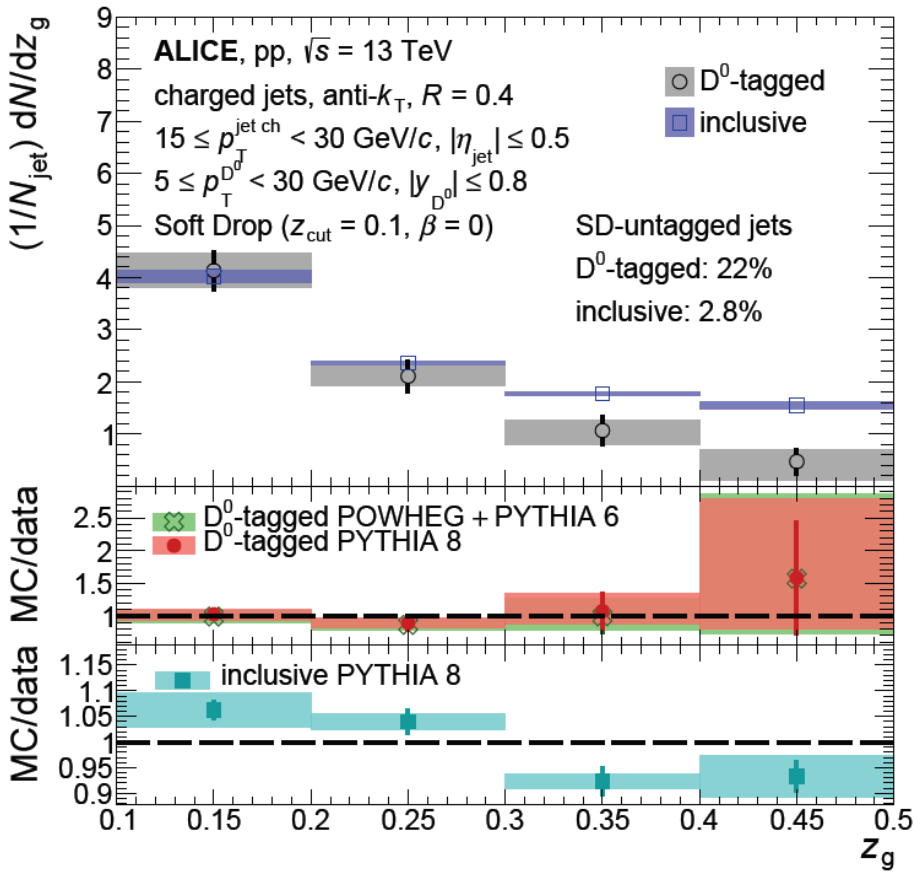

- Splitting functions describe the emission probability of partons in parton showers
  - Universal property of QCD

- Soft Drop grooming procedure:

$$z \equiv \frac{\min(p_{\mathrm{T},1}, p_{\mathrm{T},2})}{p_{\mathrm{T},1} + p_{\mathrm{T},2}} > z_{\mathrm{cut}} \left(\frac{\Delta R_{1,2}}{R}\right)^{\beta}$$

A. J. Larkoski et al. JHEP 05 (2014) 146

- Steeper splitting function for charm quarks compared to gluons and light quarks
- Model predictions for charm-quark jets describe well these measurements

"Measurements of groomed-jet substructure of charm jets tagged by D^0 mesons in proton-proton collisions at $\sqrt{s}$ = 13 TeV" (CDS / arXiv:2208.04857)

Υ production at forward rapidity

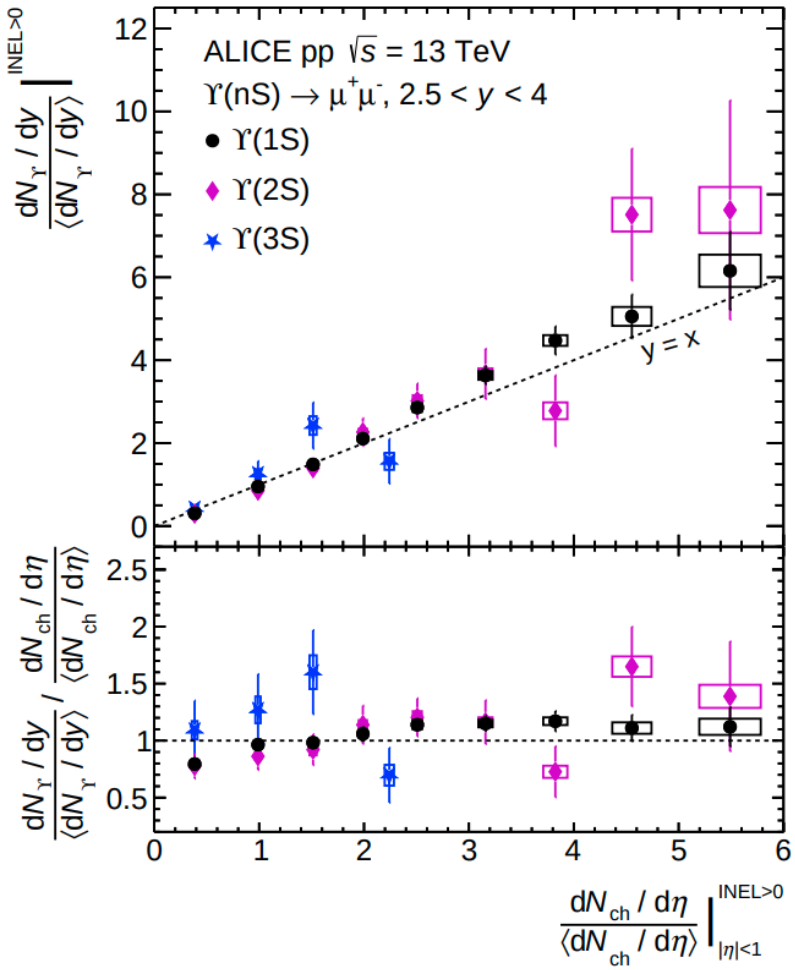

- Production of Y(1S), Y(2S) and Y(3S) exhibits a linear scaling with multiplicity
- Ratio of excited- to ground-state yields is compatible with unity
- Due to limited statistics, the suppression of Y(2S) and Y(3S) in high-multiplicity events can be neither confirmed nor excluded – to be revisited in Run 3

"Multiplicity dependence of Y production at forward rapidity on pp collisions at $\sqrt{s}$ = 13 TeV"

(CDS / arXiv:2209.04241)

EM calorimeter performance paper

- Detailed studies of the performance for different observables in various datasets
- Improved understanding of the detector response

- Highlights
  - Isolated photon reconstruction in Pb–Pb collisions
  - Reconstruction of π^0s up to 200 GeV using merged showers

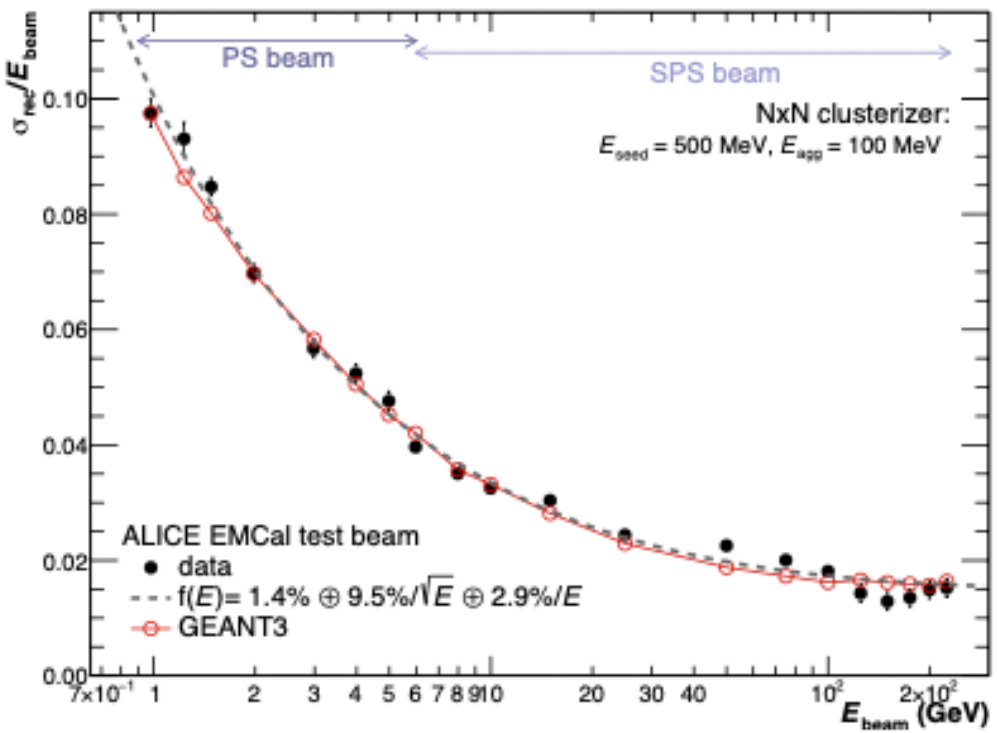

"Performance of the ALICE Electromagnetic Calorimeter" (CDS / arXiv:2209.04216)

EM calorimeter performance paper

- Detailed studies of the performance for different observables in various datasets
- Improved understanding of the detector response

- Highlights
  - Isolated photon reconstruction in Pb–Pb collisions
  - Reconstruction of π^0s up to 200 GeV using merged showers

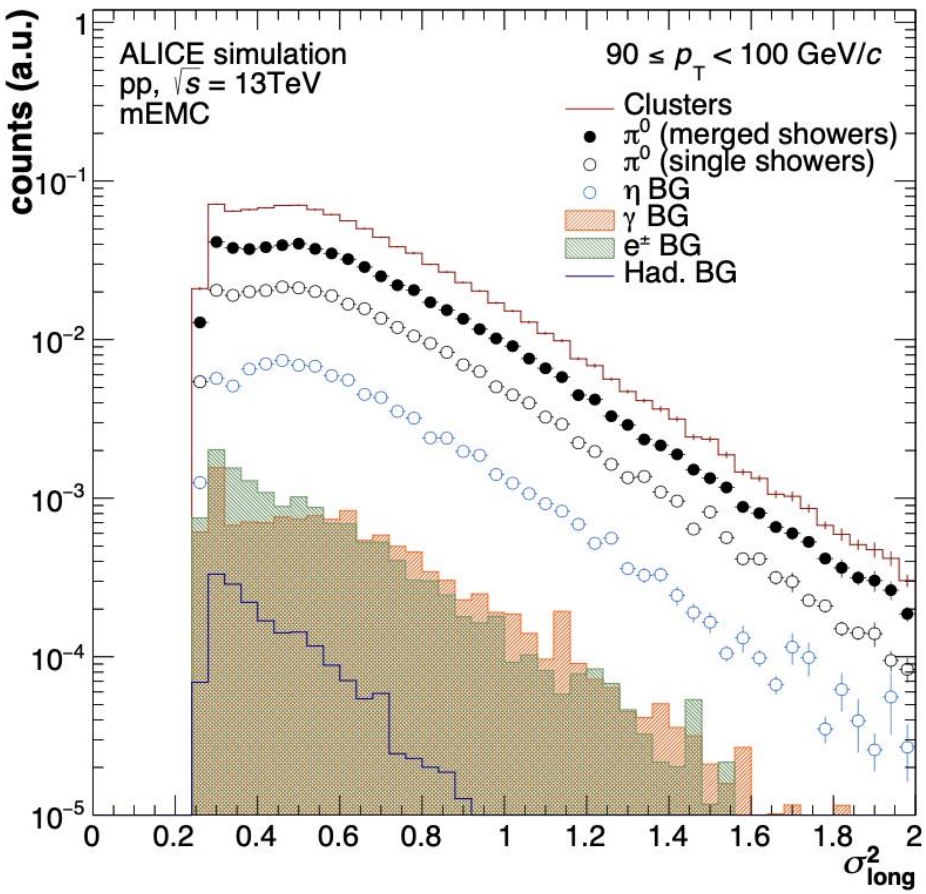

"Performance of the ALICE Electromagnetic Calorimeter" (CDS / arXiv:2209.04216)

Run 3

First collisions at 13.6 TeV

- ALICE took data successfully in production conditions

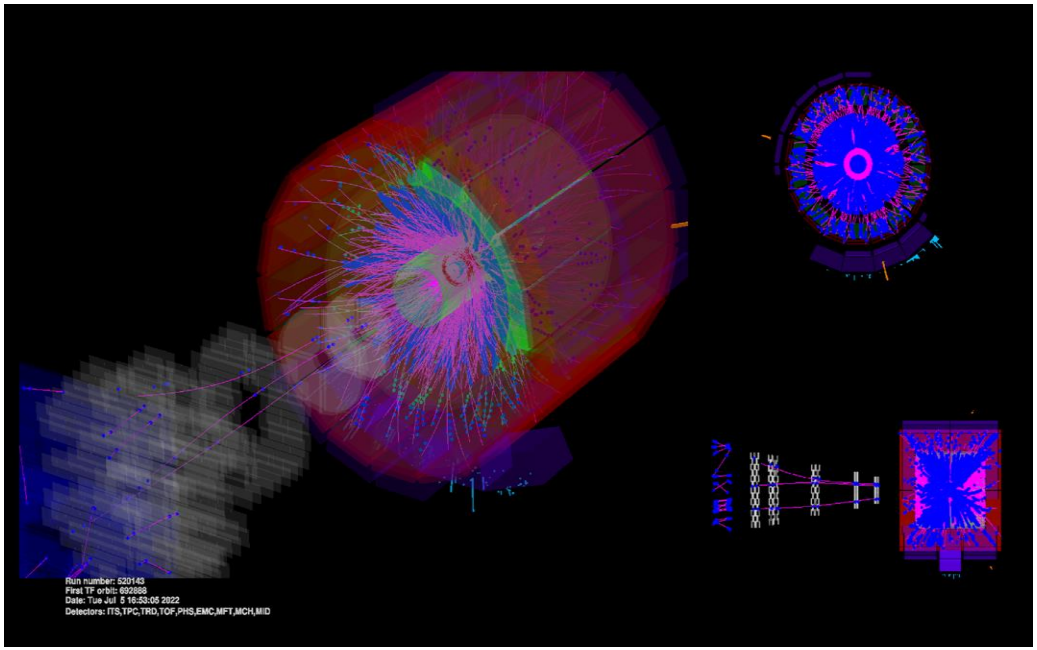

pp data taking at 500 kHz

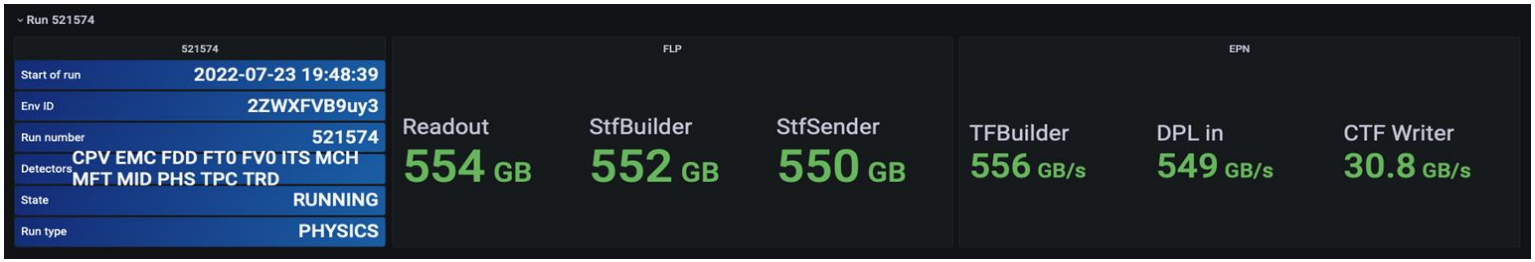

- **Detector stable in continuous readout**

- **All components integrated**
  - Detector Control, Readout
  - Synchronous reconstruction for data compression (factor 18)
  - Optimisation of the readout to reconstruction interface
  - Calibrations online and standalone
  - Central Trigger Processor
  - New firmware for improved zero suppression

- **Special runs**
  - TPC magnetic field and high-voltage scans for calibration
  - B=0 data taking for alignment
  - Low rate scan from 600 Hz to 1 MHz to study detector response

pp data taking at 500 kHz

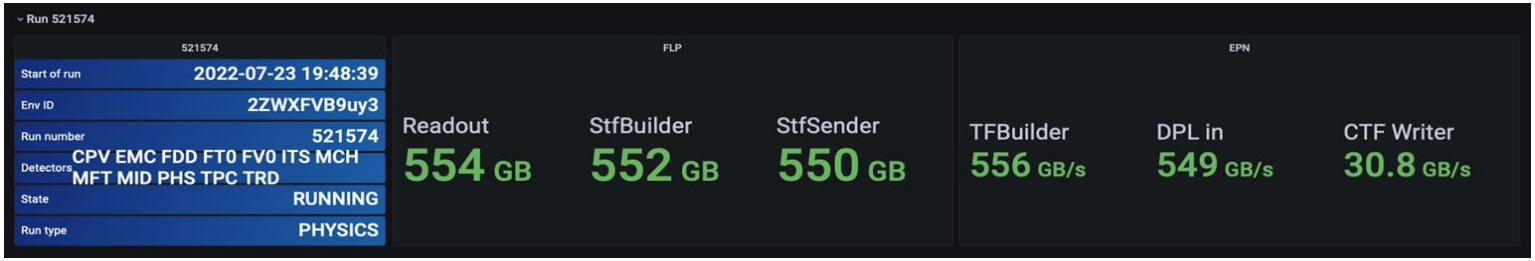

- **9.4 pb^{-1} delivered luminosity to ALICE**
  - 2×10^{12} FT0VX counts under asynchronous processing
- **Good data quality**

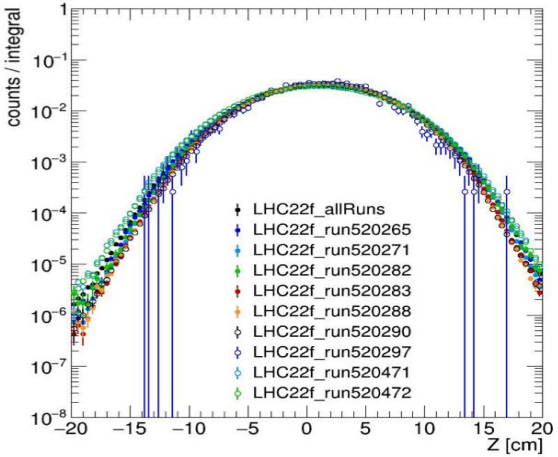

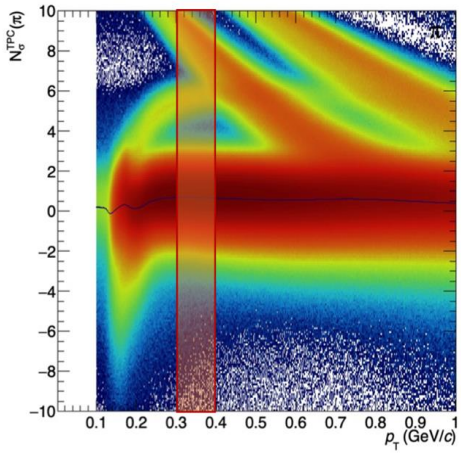

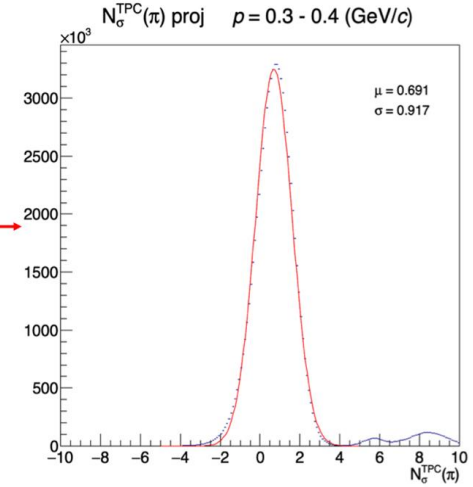

HI preparation

DONE
to be repeated

- **High-rate scans 1/2/3/4 MHz**
  - Trip rate of TPC GEM chambers reduced by optimising their functional parameters
  - Muon Chamber trip rate reduced by adding water vapour in the gas mixture
  - Other detectors stable
  - Online reconstruction and data compression stress test

ONGOING

- **Optimization of FIT front-end cards**
  - To better cope with larger dynamic rage of HI collision signal
  - To be done in TS1

- **Zero Degree Calorimeter commissioning**
  - Full readout chain with photomultiplier validated with laser
  - Integrated into the detector control system (operate hardware and levelling platform)
  - Quality control and online calibration under integration and commissioning

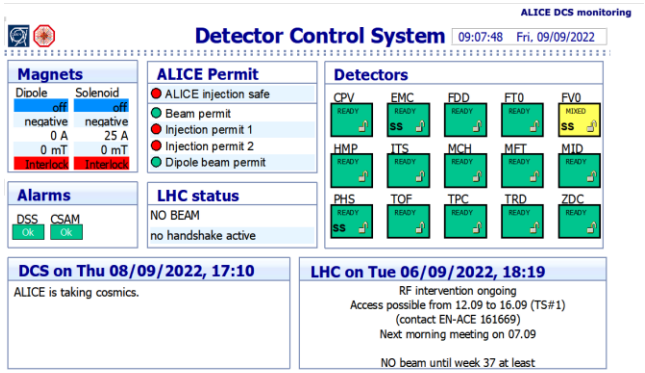

To be finalized with pp beam

Restart plans before HI

- Perform **full rate scans up to 5 MHz** to validate detector stability
- Validate the **full-fledged TPC FW** with final format and ion tail cancellation
- **Fully commission ZDC with pp beam using LHCf run** (low intensity, sparse filling schema and crossing angle < 100 urad)
- ALICE commissioning on track with respect to the original LHC schedule

- **Possible advancement of EYETS to week 48**
- Several scenarios being worked out for 2022 HI run
- HI run energy under evaluation from the results of crystal collimation in pp

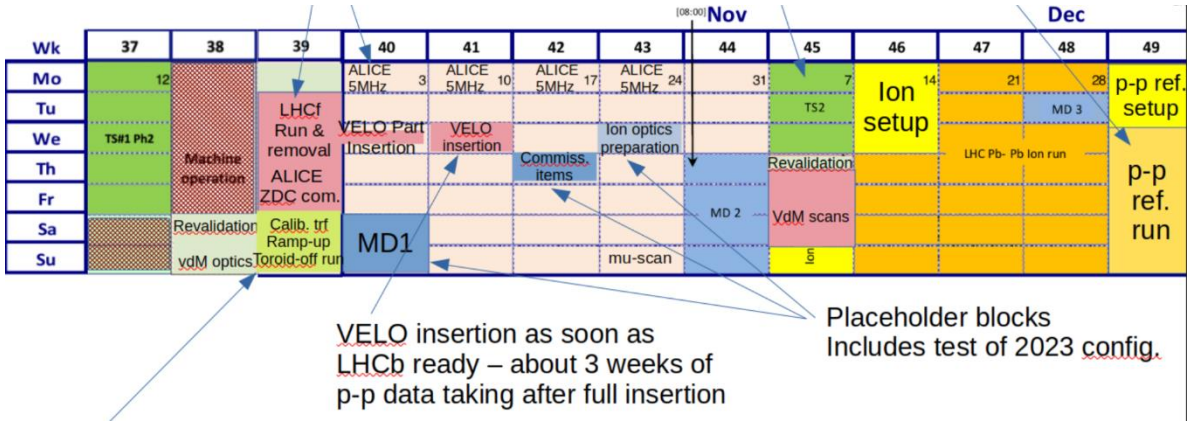

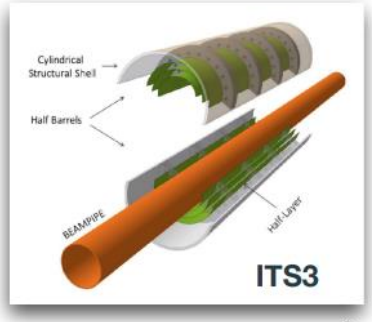

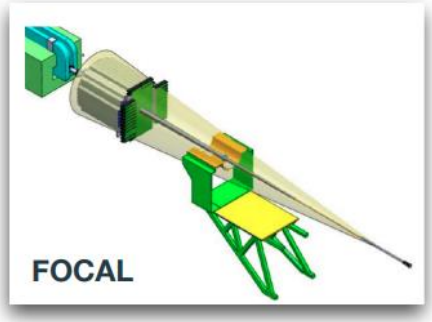

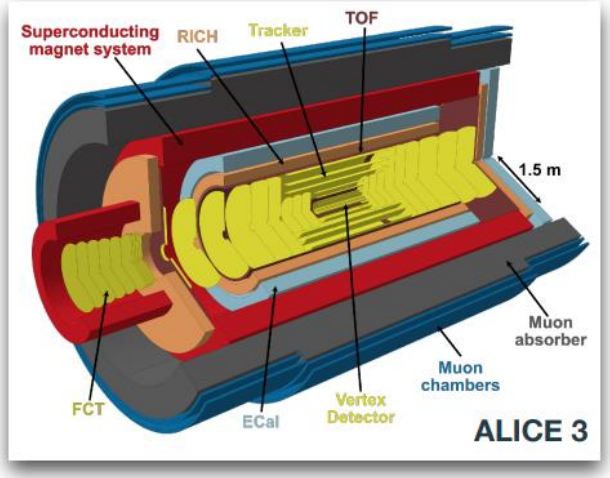

Future upgrades

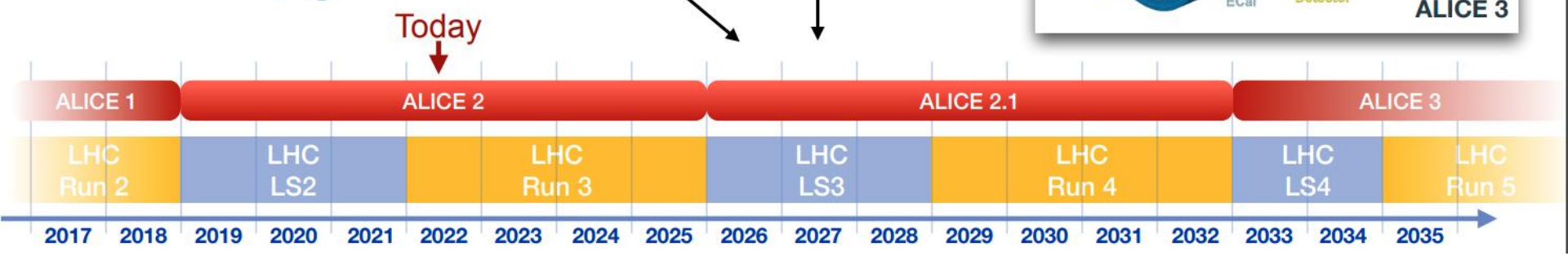

Forward calorimeter project

Letter-of-Intent: CERN-LHCC-2020-009

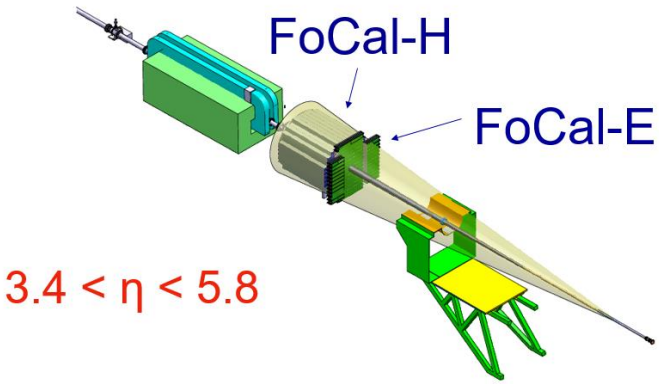

Transverse shower profile

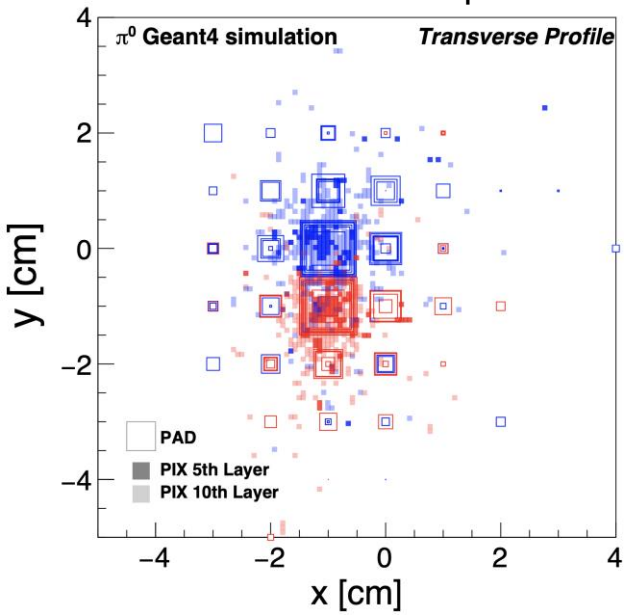

- Si-W ECAL with pixel and pad layers
  - High-granularity layers for 2-shower separation
- Cu-SciFi spaghetti HCAL
- Prototype tests at PS and SPS
  - Demonstrate technology
  - Verify performance

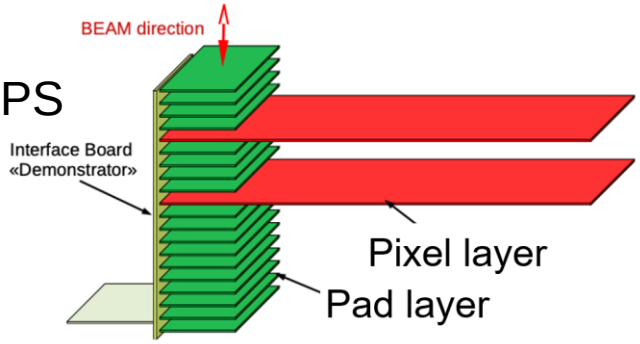

Complete pad layer setup

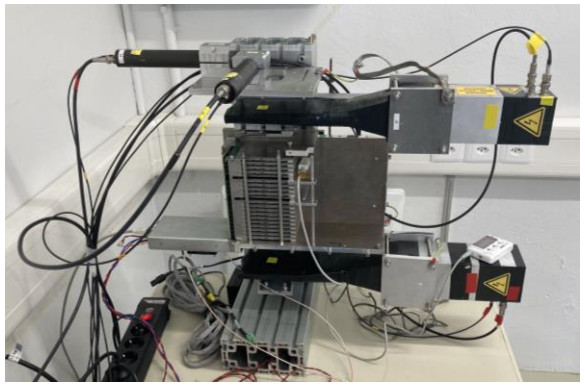

FoCal development and test beams

- Prototype test beam campaign
- PS test beam status June 2022
  - Calibrated and tuned 18 pad layers
  - Successful large scale readout
  - Further analysis ongoing
- SPS test beam goals Sept 2022
  - Determine FoCal-E energy resolution at high energy
  - Combined readout of pixel and pad layers
  - Full scale FoCal-H prototype (9 towers)

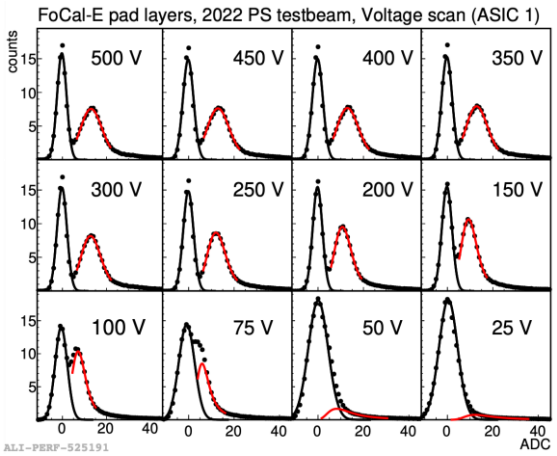

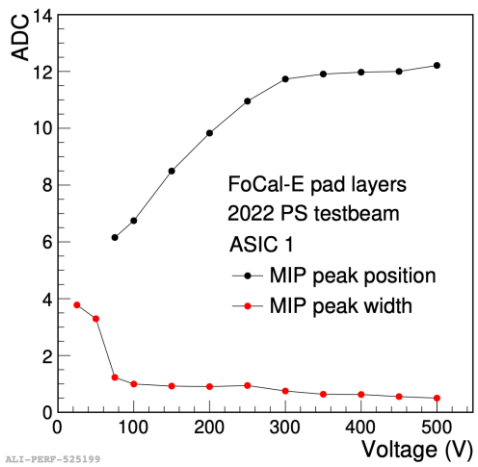

Pad layer voltage scan

New HCAL prototype

ITS3 – Mechanical integration

Engineering models 2+3

- Successful integration of second engineering model based on dummy silicon
- Now focus on:
  - interconnection
  - air distribution

engineering model 2

FPC design

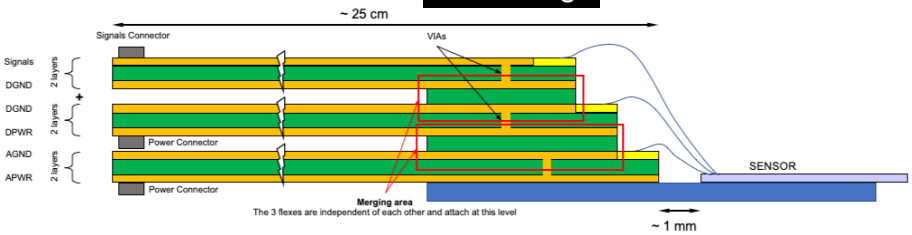

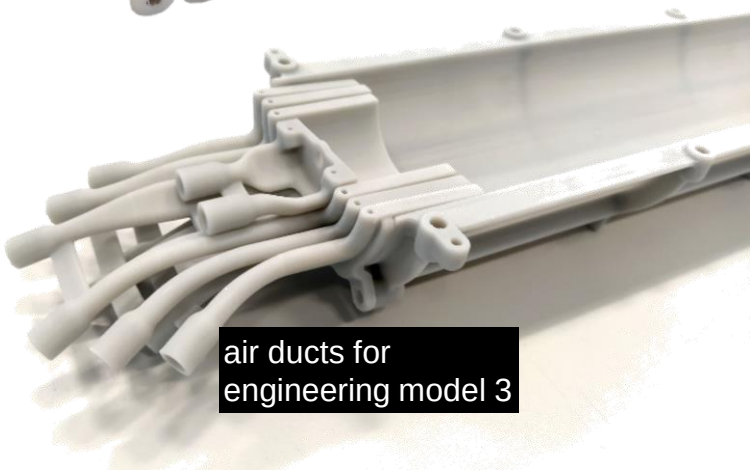

air ducts for engineering model 3

MAPS in TPSCo 65 nm technology

Test beam results from prototypes “MLR1”

- Extensive test beam campaigns with ~1 beam/month
- Qualified 65 nm process at ALICE radiation levels
  - and even up to 10^{15} 1 MeV n_{eq}/cm^2

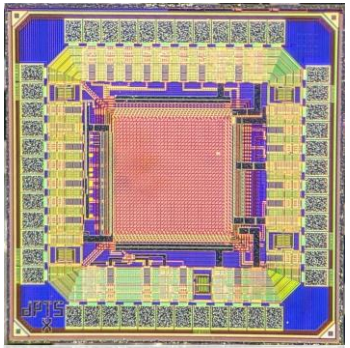

DPTS — 32x32 pixel prototype

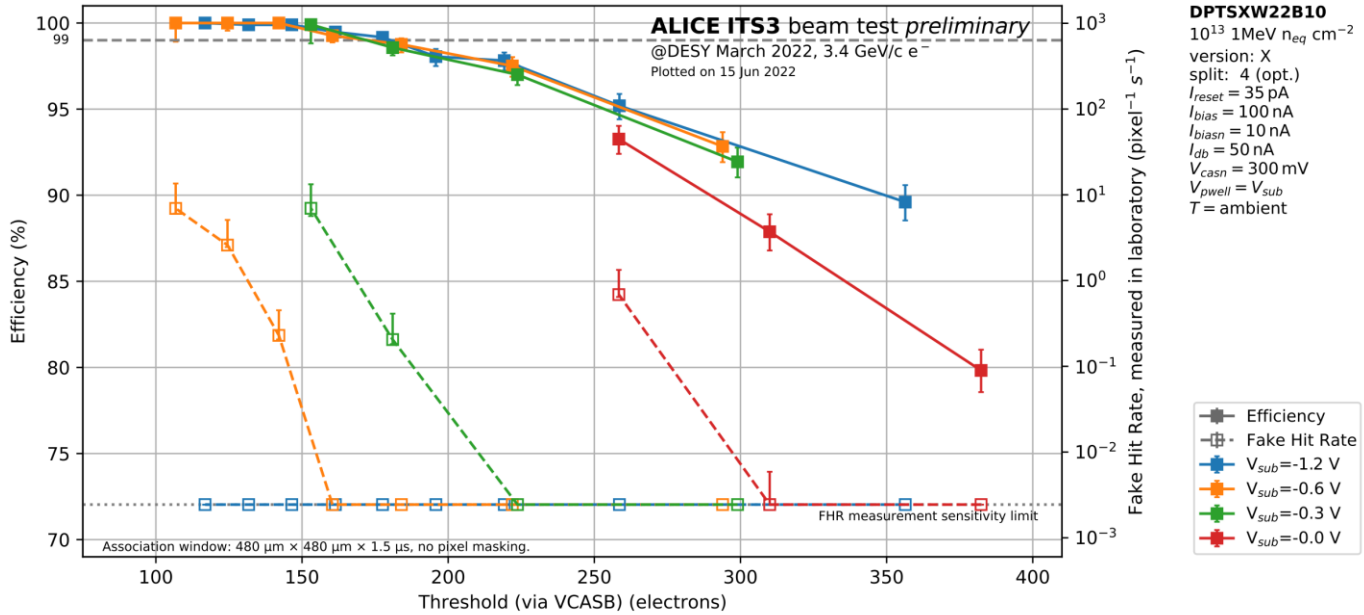

65 nm chips

Wafer-scale chip

- Next step after successful small-scale prototypes: wafer-scale chip
- Design of first wafer-scale sensors is finalising, **close to submission** for production
- Test system is under preparation

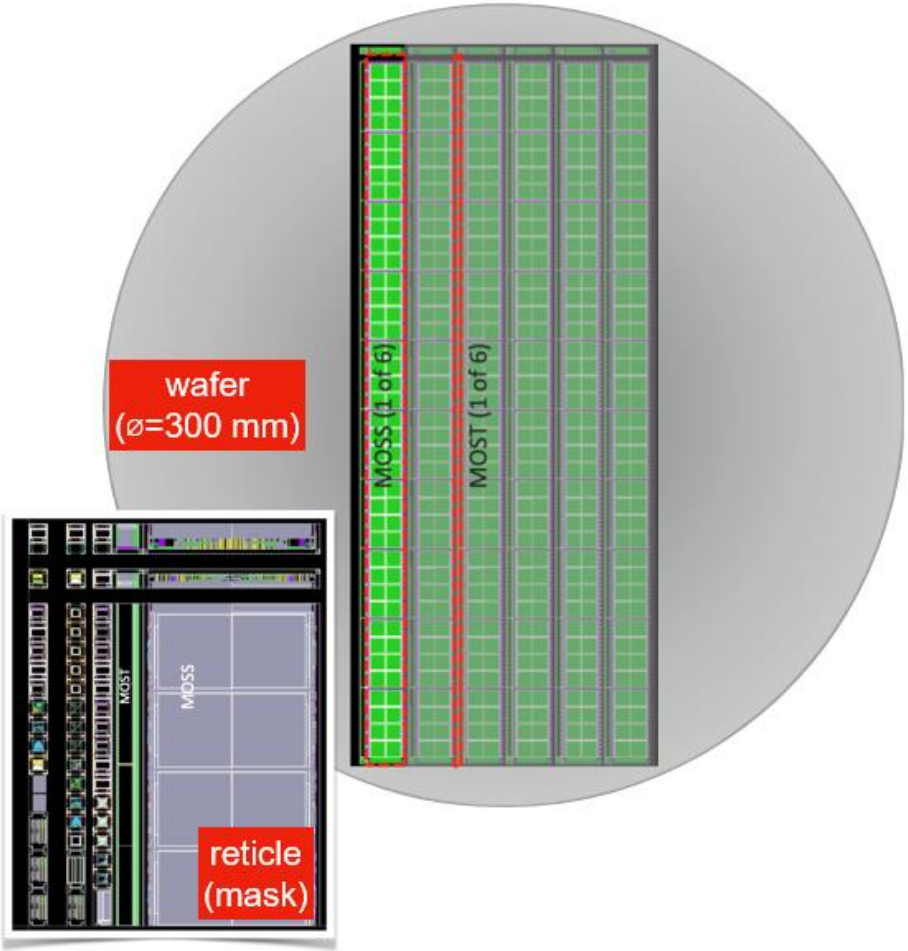

ALICE 3: Heavy ions in Run 5 & 6

- Setting up extensive R&D programme to achieve
  - ultimate pointing resolution
  - tracking with large η acceptance
  - excellent particle identification over full acceptance

- Pushing technologies of general HEP interest
  - monolithic silicon pixel sensors
  - silicon timing sensors
  - silicon photosensors
  - minimal material budget: optimised powering and mechanical integration

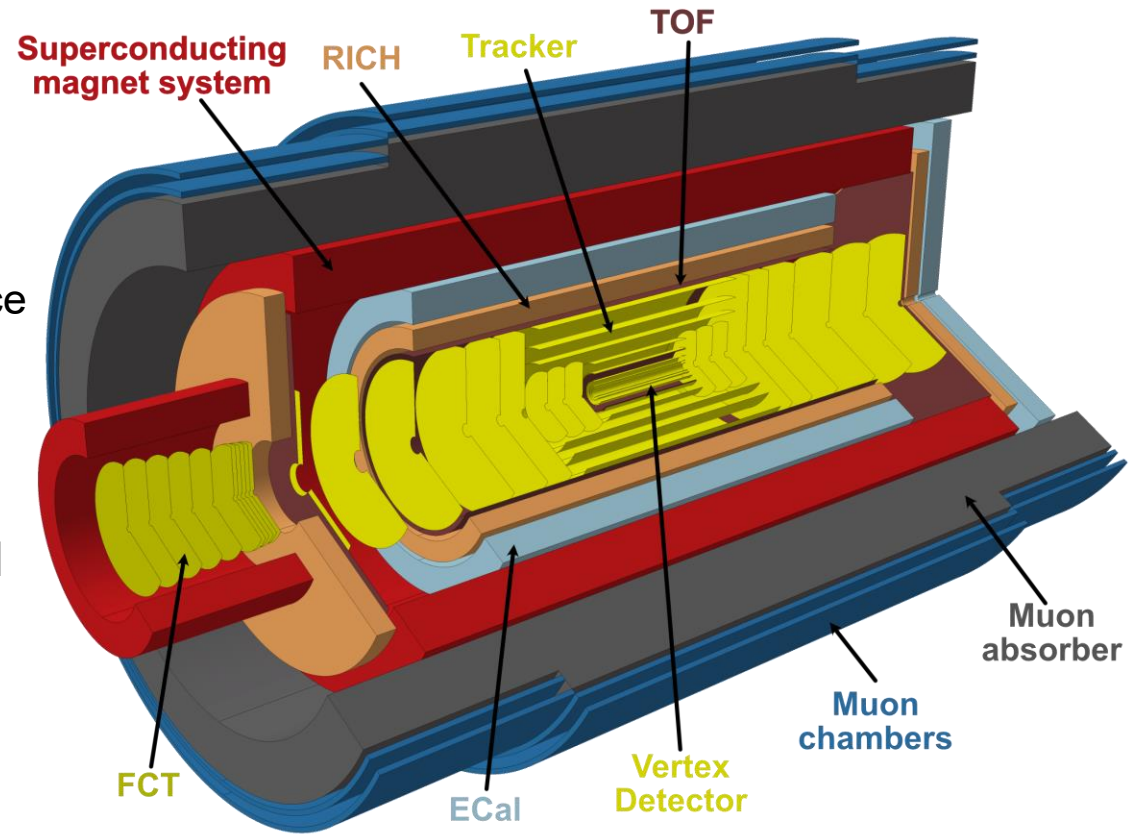

- **ALICE upgrade week in Prague (Sep 19–23)** to discuss R&D activities and plans

Thanks!

Backup slides

Charm-quark splitting function

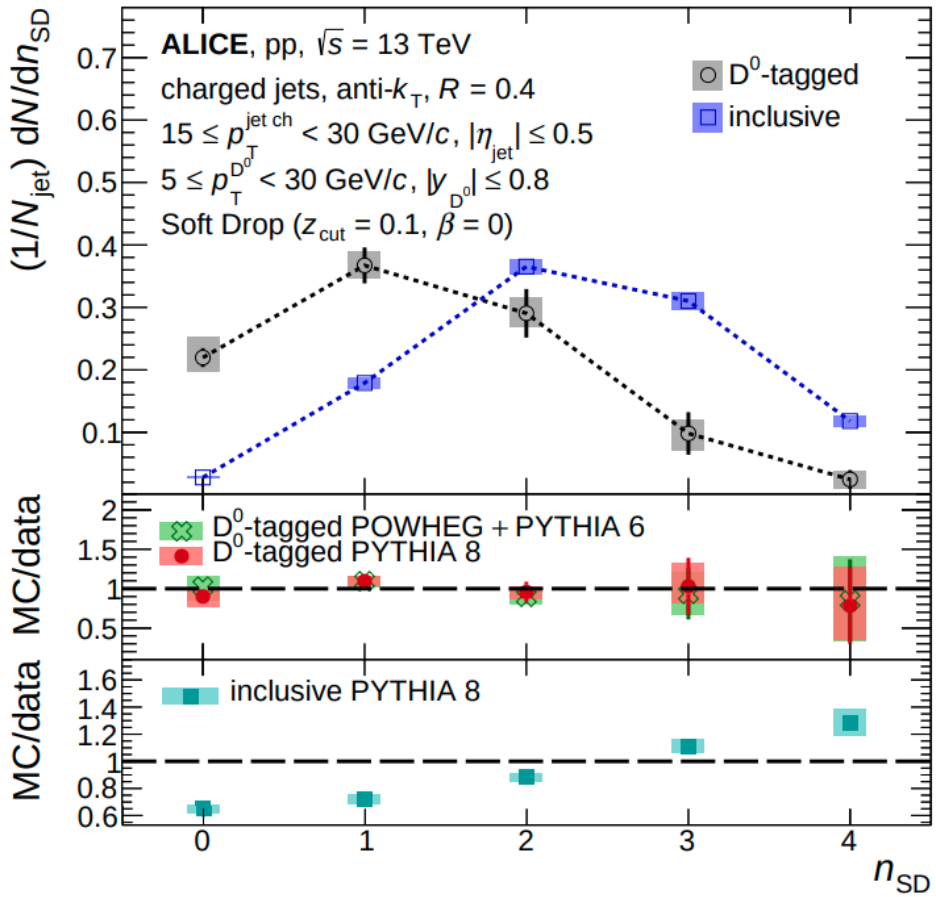

- Distribution of number of splittings – clear shift in distribution
- Charm has less hard splittings – more of original energy is kept
  - Consistent with dead-cone effect

    Nature 605 (2022) 440-446
- Harder fragmentation for charm quarks

"Measurements of groomed-jet substructure of charm jets tagged by D^0 mesons in proton-proton collisions at $\sqrt{s}$ = 13 TeV" (CDS / arXiv:2208.04857)

Lower-order contributions

Data-driven method

- Use event mixing
- Two particles from the same event and one particle from another:

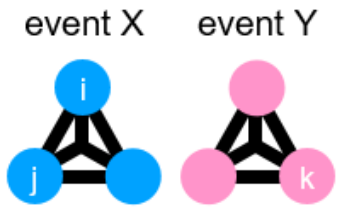

$$C_{ij}([\mathbf{p}_i,\mathbf{p}_j],\mathbf{p}_k) = \frac{N_2(\mathbf{p}_i,\mathbf{p}_j)N_1(\mathbf{p}_k)}{N_1(\mathbf{p}_i)N_1(\mathbf{p}_j)N_1(\mathbf{p}_k)}$$

- Calculate Lorentz-invariant scalar Q_3 for every triplet $\mathbf{p}_i, \mathbf{p}_j, \mathbf{p}_k$ to obtain $C_{ij}(Q_3)$

$$Q_3 = \sqrt{-q_{ij}^2 - q_{jk}^2 - q_{ki}^2}$$

Projector method

- Use two-particle measured or theoretical correlation function $C([\mathbf{p}_i,\mathbf{p}_j])$
- Perform kinematic transformation:

$C_2(k_{ij}^*) \rightarrow C_{ij}(Q_3)$

$k_{ij}^*\,(pair) \rightarrow Q_3\,(triplet)$

For one Q_3 value

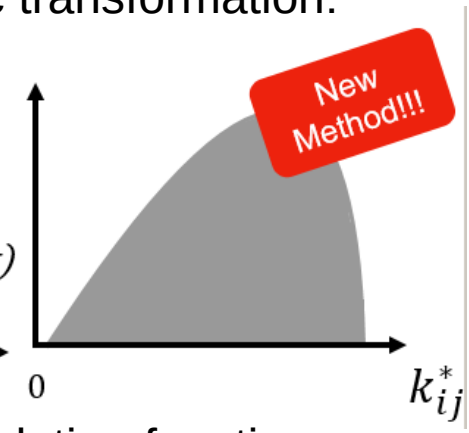

- To obtain the correlation function

$$C_{ij}(Q_3) = \int C(k_{ij}^*) W_{ij}(k_{ij}^*, Q_3) dk_{ij}^*$$

Del Grande et al. EPJC 82 (2022) 244

"Towards the understanding of the genuine three-body interaction for p−p−p and p−p−Λ"
(CDS / arXiv:2206.03344)

Flow of identified hadrons

- Elliptic flow estimated with 4-particle cumulants, $v_2\{4\}$, for identified hadrons:

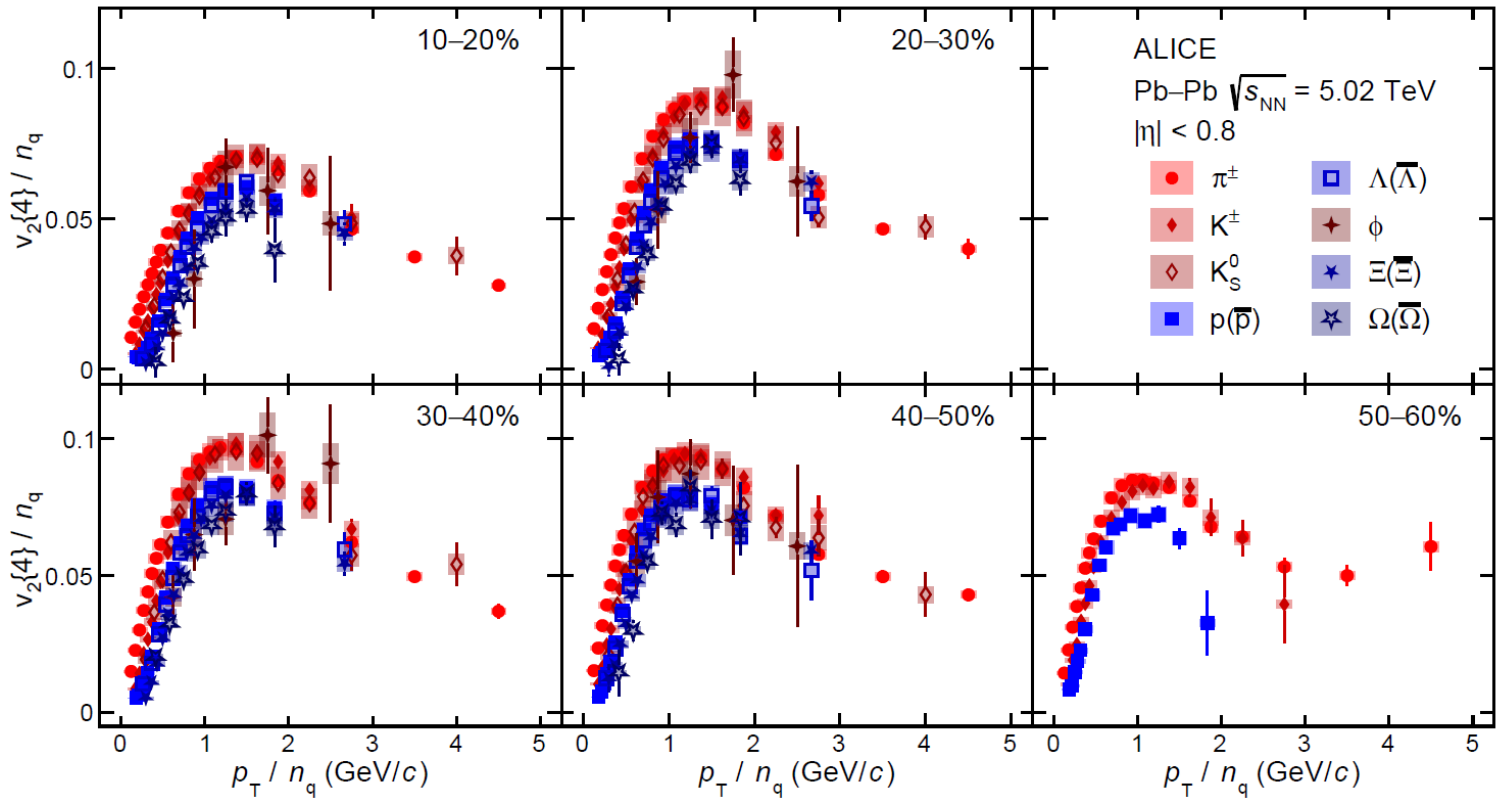

- Only approximate (within ~20%) number of constituent quark (NCQ) scaling at LHC

"Anisotropic flow and flow fluctuations of identified hadrons in Pb−Pb collisions at $\sqrt{s_{NN}}$ = 5.02 TeV" (CDS / arXiv:2206.04587)

Femtoscopic technique: 3-body

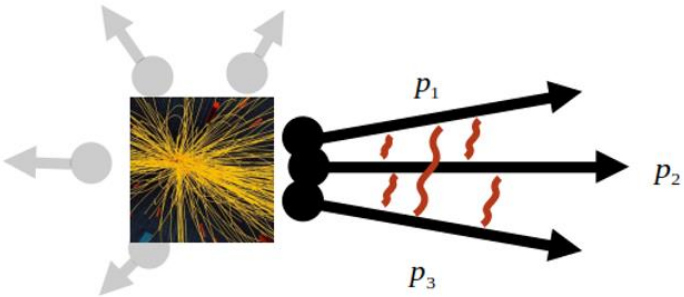

Three-particle correlation function

$$C(p_1, p_2, p_3) \equiv \frac{P(p_1, p_2, p_3)}{P(p_1)P(p_2)P(p_3)} = N \frac{N_{\text{same}}(Q_3)}{N_{\text{mixed}}(Q_3)}$$

$$Q_3 = \sqrt{-q_{ij}^2 - q_{jk}^2 - q_{ki}^2}$$

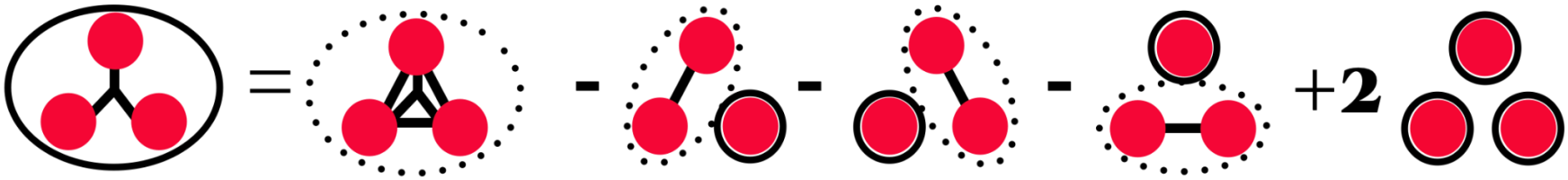

Genuine 3-body correlation

3-body correlation

2-body correlation + permutations

Non-interacting particles

Flow fluctuations

- Relative elliptic flow fluctuations of identified hadrons:

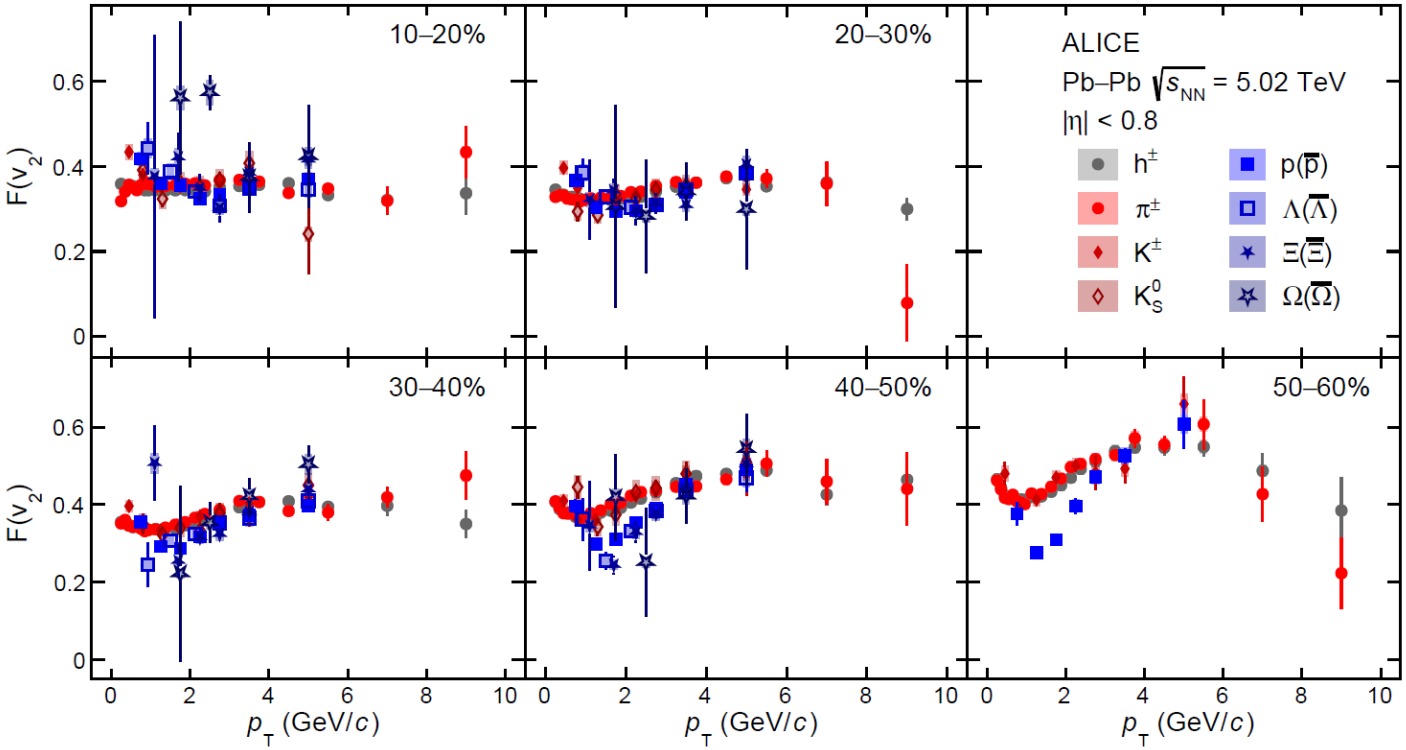

$$\langle v_n \rangle \approx \sqrt{\frac{v_n^2\{2\} + v_n^2\{4\}}{2}}$$

$$\sigma_{v_n} \approx \sqrt{\frac{v_n^2\{2\} - v_n^2\{4\}}{2}}$$

$$F(v_n) = \frac{\sigma_{v_n}}{\langle v_n \rangle}$$

- Not-trivial dependence only in peripheral collisions
  - Splitting between baryons and mesons

"Anisotropic flow and flow fluctuations of identified hadrons in Pb−Pb collisions at $\sqrt{s_{NN}}$ = 5.02 TeV" (CDS / arXiv:2206.04587)